Journal of Engineering Physics and Thermophysics, Vol. 77, No. 4, 2004

DYNAMICS OF GROUND HEAT STORAGE AND CHOICE OF RATIONAL SOLUTIONS

A. I. Nakorchevkii

UDC 662.995+536.242

An integral method for solving problems of nonstationary heat conduction is proposed. This method can be used for mathematical modeling of the dynamics of heat storage in an unbounded ground mass with the use of individual heat exchangers positioned upright in the ground or a group of heat exchangers. The influence of regular, long interruptions in the operation of heat exchangers, which often happen in solar power engineering, on the heat-storage process has been considered. It has been established that this process should be controlled, individual heat exchangers should be provided with intermediate twenty-four-hours' heat storage devices, and the work of individual heat exchangers is not very efficient. The calculations have shown that the conditions of heat storage become better in the case of group deposition of several heat exchangers.

Introduction. Since the power resources of the depths of the earth are limited, it is necessary to find alternative energy sources: from waste heat recovery to the conversion of solar energy into heat. If the thermodynamic potential of nonconventional power sources is small, they can be used in systems providing public needs (heating and hot-water supply) that consume energy very irregularly during the year. In this case, it is necessary to solve the problem of storage of heat in the summer–autumn period and its subsequent consumption in the winter–spring time. One of the objects that can be used for energy storage is a natural ground mass with heat- exchangers positioned in it. Diagrams of typical heat exchangers are presented in Fig. 1. The heat-exchanger surface Z interacts with the ground. The heat-exchange surface H with outside diameter R_0 is heat-insulated. The bulk of the energy is stored in the volume $V(t)$, the upper elevation of which $h(t)$ should be lower than the elevation of the mass surface. In the case where U-shaped heat exchangers are used, their temperature substantially levels off along the height z because of the counterflows of one and the same heat-transfer agent in the downward and upward branches. Such an effect will also occur in a coaxial heat exchanger if the thermal resistance of the separating wall is small. Therefore, it may be assumed that heat propagates in the ground predominantly in the radial direction and the basic equation of its conservation has the form

$$\frac{\partial T}{\partial t} = a_{\text{m}} \left(\frac{\partial^2 T}{\partial r^2} + \frac{i-1}{r} \frac{\partial T}{\partial r} \right) \quad (i = 1, 2, 3) \tag{1}$$

in the plane, cylindrical, and spherical coordinate systems (depending on the value of i). Representation (1) does not exclude the possibility of change in the temperature along the height z in accordance with the boundary conditions that are determined by the regime of operation of the heat exchanger and can change arbitrarily or even be interrupted when it begins or ceases to operate.

1. Computational Relations. At present, there is no exact analytical solution of (1) for the case of arbitrary boundary conditions [1]. Therefore, the challenge is to find a system that would be equivalent (or almost equivalent) to Eq. (1) and its solution that would satisfy the boundary conditions of heat storage. In this case, it is necessary to take into account the characteristic features of Eq. (1) in the region of determination of functions: first, classical solutions of (1) are found in the form of infinite series leading to cumbersome dependences; second, the region of determination of functions is infinite; third, in accordance with (1), the velocity of propagation of temperature perturbations is infinitely high even though it is finite in actual fact. These features can be called the problems of "three infinities."

Institute of Technical and Thermal Physics, National Academy of Sciences of Ukraine, 2a Zhelyabov Str., Kiev, 03057, Ukraine. Translated from Inzhenerno-Fizicheskii Zhurnal, Vol. 77, No. 4, pp. 10–19, July–August, 2004. Original article submitted April 24, 2003; revision submitted October 28, 2003.

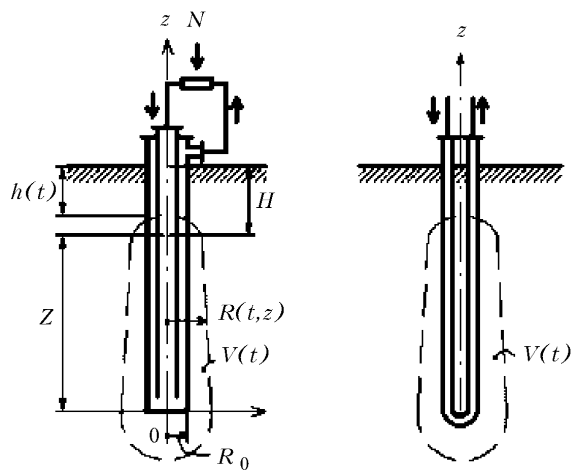

Fig. 1. Diagrams of coaxial and U-shaped heat exchangers.

The problem of the "first infinity" has been successfully solved in [2] by introduction of a highly exact, universal, one-parameter interpolation series of functions of temperature distribution in bodies of standard shape, such as a plate, cylinder, or sphere. This method, going back to the Kármán–Pohlhausen ideas [3], can also be used for solving the second problem and, partially, the third problem in the case where the functions at a finite distance $R(t, z)$ are assigned their values at infinity:

$$r = R_0 : \quad T = T_0 , \quad \frac{\partial T}{\partial r} = -\frac{q_0}{\lambda_m} ;$$
$$r = R : \quad T = T_m , \quad \frac{\partial T}{\partial r} = 0 , \quad \frac{\partial^2 T}{\partial r^2} = 0 . \tag{2}$$

The third condition in (2) follows from (1) at $\partial T_m / \partial t = 0$. Taking into account (2), we may write a universal (common for i = 1, 2, and 3) one-parameter series of functions:

$$\frac{T - T_m}{T_0 - T_m} = (1 - \eta)^3 \, (1 + 3\eta - A_m \eta) , \tag{3}$$

where

$$\eta = \frac{r - R_0}{R - R_0} ; \quad A_m = \frac{q_0 \, (R - R_0)}{\lambda_m \, (T_0 - T_m)} ; \quad q_0 = \alpha_0 \, (T_w - T_{i.s}) . \tag{4}$$

From the expression for the parameter A_m, we obtain the Biot criterion

$$\mathrm{Bi}_m = \frac{\alpha_0 \, (R - R_0)}{\lambda_m} , \quad A_m = \mathrm{Bi}_m \, \frac{T_w - T_{i.s}}{T_0 - T_m} . \tag{5}$$

The physical meaning of A_m is the ratio between the temperature gradient in the ground at $r = R_0$ and its average value in the heat-storing mass. The dependence (3) is true for the region $0 \le A_m \le +4$. To derive formulas of the type of (3) where $A_m > +4$, we note that

$$A_m = 3 \Rightarrow \frac{T - T_m}{T_0 - T_m} = (1 - \eta)^3 = (1 - \eta)^{A_m} , \quad A_m = 4 \Rightarrow \frac{T - T_m}{T_0 - T_m} = (1 - \eta)^4 = (1 - \eta)^{A_m} . \tag{6}$$

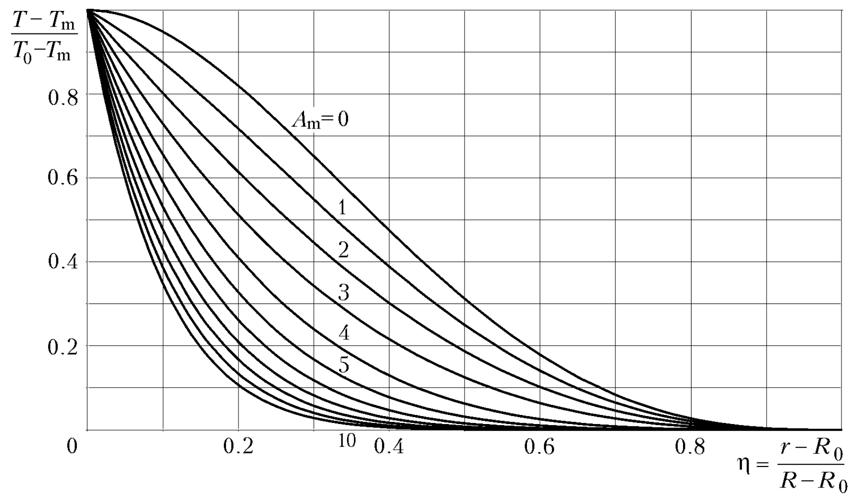

Fig. 2. Temperature distributions in the ground mass at different values of A_m.

A recursion continuation of (3) suggests itself:

$$\frac{T - T_m}{T_0 - T_m} = (1 - \eta)^{A_m} , \tag{7}$$

if $+4 < A_m \le +\infty$. Dependence (7) satisfies conditions (2). The temperature distributions calculated by (3) and (7) are presented in Fig. 2. Since the real temperature distributions in the process of heat storage in a ground mass can be thought of as smooth and monotone in the direction r, formulas (3) and (7) can be considered as fairly exact if they strictly satisfy the five conditions at the boundaries of the interpolation region (by analogy with the results of comparison of particular exact solutions with analogous dependences in [2]).

According to (3)–(7), to solve the problem considered at given $T_m(z)$ and $\lambda_m(z)$ it is necessary to find the following six functions:

$$T_w(t, z) , \quad T_{i.s}(t, z) , \quad T_0(t, z) , \quad R(t, z) , \quad \alpha_0(t, z) , \quad A_m(t, z) . \tag{8}$$

These functions can be determined with the use of:

(1) the equation of conservation of energy of the heat-transfer agent

$$\frac{\partial T_w}{\partial z} = -2\pi R_{i.s} \frac{\alpha_{i.s}(T_w - T_{i.s})}{G_w c_w} ; \tag{9}$$

(2) the equation of heat transfer through the wall of the heat exchanger

$$T_{i.s} = \frac{\alpha_{i.s} T_w + p_{i.s} T_0}{\alpha_{i.s} + p_{i.s}} , \quad p_{i.s} = \frac{\lambda_{i.s}}{R_{i.s} \ln \left(\frac{R_0}{R_{i.s}} \right)} ; \tag{10}$$

(3) the equation of change in the temperature of the ground mass at $r = R_0$, following from the basic Eq. (1) and formulas (3) and (7),

$$\frac{\partial T_0}{\partial t} = -a_m \frac{T_0 - T_m}{R - R_0} \left[\frac{6(2 - A_m)}{R - R_0} + \frac{(i-1) A_m}{R_0} \right] \text{ at } A_m \in [0; +4] ,$$

$$\frac{\partial T_0}{\partial t} = -a_m \frac{T_0 - T_m}{R - R_0}\left[\frac{A_m(1 - A_m)}{R - R_0} + \frac{(i-1)A_m}{R_0}\right] \text{ at } A_m \in [+4; +\infty]\ ; \tag{11}$$

(4) the equation of conservation of the energy stored in the ground Ei(t)

$$\int_0^t dt \int_0^Z 2\pi R_0 q_0 dz = \int_0^Z dz \int_{R_0}^R 2\pi\rho_m c_m (T - T_m)\, r dr + \int_{R_0}^{R(0)} 2\pi\rho_m c_m (T - T_m)\, r^2 dr + \int_{R_0}^{R(Z)} 2\pi\rho_m c_m (T - T_m)\, r^2 dr\ , \tag{12}$$

where $(T - T_m)$ is determined from (3) or (7) and the heat-flux density q_0 at $r = R_0$ is determined from the expression for q_0 in (4);

(5) the expression for A_m in (4);

(6) the heat-transfer coefficient $\alpha_{i.s}$ on the wall with $r = R_{i.s}$

$$\alpha_0 = \alpha_{i.s}\left(\frac{R_{i.s}}{R_0}\right)^{i-1}\ , \tag{13}$$

which is determined as a result of the combined solution of the heat and hydrodynamic problems with the use of known dependences for the heat exchangers considered.

Thus, the system of integral, differential, and algebraic equations is closed and the following boundary conditions are set:

$$T(0, r) = T_m(z)\ ,\quad R(0, z) = R_0\ ,$$

$$T(t, \infty) = T_m(z)\ ,\quad T(t, R_0) = T_0(t, z)\ ,\quad \left(\frac{\partial T}{\partial r}\right)_{r=R_0} = -\frac{q_0(t, z)}{\lambda_m} \tag{14}$$

It should be noted that Eq. (11) is true for the conditions at the boundary of the region of determination of the problem.

2. Analysis of Operation of an Individual Heat Exchanger. As was noted above, the operation of heat exchangers can be interrupted in the process of heat storage. These interruptions are especially long in the case of solar energy storage because of the small duration of a light day (about eight hours) and the existence of clouds. The calculations presented below were done for a conditional ten-day-period cycle including eight hours of operation of solar-energy collectors during a continuous sequence of eight days and two nonworking days. Three ten-day periods represent a month and six months represent an interruption in the seasonal heat storage. During the interruptions, the value of the heat flow changes abruptly — from the maximum to zero and inversely. Since the rate of propagation of temperature perturbations is high (theoretically infinite), the temperature profile changes almost instantaneously in the region $R_0 \le r \le R$ in response to an instantaneous change in the quantity A_m at R = idem and Ei = idem. When heat supply is terminated because of the maximum "filling" of the temperature profile at $A_m = 0$ (see Fig. 2), T_0 decreases abruptly and then the stored heat begins to continuously drift (Ei = const) and $R(t, z)$ increases. The rate of change in T_0 and R is determined by Eqs. (11) and (12) at $A_m = 0$. The next introduction of heat into the ground leads to an equally abrupt increase in A_m and T_0.

Table 1 presents the conditions of heat storage at its initial stage, calculated at the following parameters of the interacting systems: a) ground, $\rho_m = 1.84 \cdot 10^3$ kg/m^3, $\lambda_m = 1.42$ W/(m·K), $c_m = 1.15 \cdot 10^3$ J/(kg·K), and $T_m = 10^{o}$C; b) coaxial heat exchanger, $R_0 = 0.054$ m, $R_{i.s} = 0.050$ m, $r_{i.s} = 0.040$, $\lambda_{i.s} = 17.5$ W/(m·K), $Z = 50$ m, $G_w = 5.0$ kg/sec, Re $= 0.67 \cdot 10^5$, $\alpha_0 = 0.86 \cdot 10^4$ W/(m^2·K), $v_w = 1.79$ m/sec, $\xi = 0.02$, and, at a constant temperature of the heat-transfer agent (water), $T_w = (T_{w,b} + T_{w,e})/2 = 50^{o}$C. The data on the temperature at the input of the heat exchanger $T_{w,b}$ point to the gradientlessness of the process along the height z. The algorithm for calculating the initial stage of heat storage, where $T_0(0, z) = T_m$, is complex and so is not presented here. We only note that the values of the quantity A_m are initially large, then they abruptly decrease and equally abruptly increase. The computer stopped the digital print-out at

TABLE 1. Change in the Conditions of Heat Storage at Its Initial Stage

t, h	$T_{i.s}$, ^oC	T_0, ^oC	R, m	A_m	q_0, W/m^2	Ei, 10^8 J	$T_{w,b}$, ^oC
0.100	49.714	49.134	0.109	2.435	2443.9	0.26387	50.992
0.200	49.781	49.338	0.134	2.672	1869.3	0.39252	50.759
0.300	49.810	49.426	0.155	2.920	1621.2	0.49830	50.658
0.400	49.827	49.476	0.176	3.230	1479.8	0.59264	50.601
0.500	49.837	49.507	0.210	3.874	1392.2	0.68010	50.565
0.600	49.844	49.528	0.250	4.641	1331.5	0.76335	50.541
0.700	49.850	49.547	0.293	5.447	1279.0	0.84301	50.519
0.800	49.855	49.562	0.346	6.418	1236.7	0.91978	50.502
0.900	49.860	49.574	0.410	7.616	1201.6	0.99421	50.488
1.000	49.863	49.585	0.492	9.140	1171.9	1.0667	50.476
1.100	49.866	49.594	0.601	11.154	1146.4	1.1374	50.465
1.200	49.869	49.602	0.752	13.950	1124.1	1.2067	50.456
1.300	49.871	49.609	0.976	18.104	1104.5	1.2748	50.448
1.400	49.873	49.615	1.345	24.942	1087.1	1.3417	50.441
1.500	49.875	49.620	2.067	38.344	1071.4	1.4076	50.435
1.600	49.876	49.625	4.131	76.607	1057.3	1.4726	50.429
1.700	49.878	49.630	60.004	1112.700	1044.4	1.5368	50.424
1.705	49.878	49.630	89.124	1652.600	1044.1	1.5384	50.424
1.710	49.878	49.630	172.890	3205.800	1043.8	1.5400	50.424
1.715	49.878	49.630	2802.100	51958.000	1043.5	1.5416	50.424

t = 1.715 h since at $t > 1.72$ h $R \to \infty$ and $A_m \to \infty$. These functions will change in a similar way in the case of use of any other types of heat exchangers and at a substantially lower heat-flow density q_0.

This seemingly unexpected result has a clear physical explanation and completely correlates with both the basic equation (1) and the features of the problem outlined in Sec. 1. Moreover, this result is also important from the practical standpoint and therefore should be considered in more detail. If the thermodynamic potential is small ($T_0 - T_m \sim 40\ ^oC$), at a heat-flow density of $q_0 \sim 10^3$ W/m^2 and a high thermal resistance of the ground ($a_m \sim 10^{-6}$ m^2), it "becomes depleted" practically completely for a short time in a small neighborhood R_* of the ground mass adjacent to the heat exchanger. The next introduction of heat into the ground under steady-state conditions (see the last four rows of the table) where the energy balance is strictly fulfilled (the integral equation (12) determining R was solved by the iteration method and the relative error of control of the integral invariability did not exceed $\pm 10^{-15}$) inevitably leads to $R \to \infty$ and $A_m \to \infty$. Such a value of R conforms well with the infinitely large rate of heat propagation. To the contrary, the small value of R_* and its practical invariability are explained by the following facts. Let $T_*(R_*)$ be determined by the value of $\Delta\bar{T}_* = (T_* - T_m)/(T_0 - T_m) \approx 10^{-2}$–$10^{-3}$, which corresponds to 99–99.9% of the $T_0 - T_m$ potential "depletion." At $A_m > 4$, in accordance with (4) and (7), we have

$$\eta_* = 1 - \Delta\bar{T}_*^{1/A_m}, \quad R_* = R_0 + \eta_* A_m \frac{\lambda_m (T_0 - T_m)}{q_0}. \tag{15}$$

The calculation by the first formula of (15) has shown that the value of the complex $\eta_* A_m$ remains practically unchanged at $A_m > 10^3$ (Fig. 3). Thus, the region of storage of energy with a potential of higher than $T_* = T_m + 10^{-3}(T_0 - T_m)$ has a radius

$$R_* = R_0 + 6.9 \cdot \frac{\lambda_m (T_0 - T_m)}{q_0}.$$

At $\lambda_m \sim 1$ W/(m·K), $T_0 - T_m \sim 40^oC$, $q_0 \sim 1000$ W/m^2, and $R_0 \sim 0.05$ m, $R_* \sim 0.31$ m, whereas $R > 40$ km. The discrepancy between the values of R_* and R is evident. Expansion of function (7) into the Taylor series and estimation

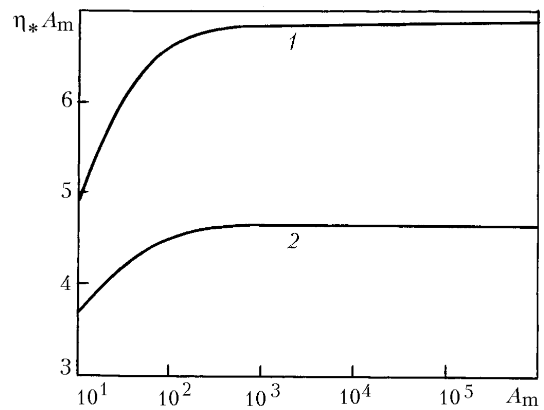

Fig. 3. Value of the complex $\eta_* A_m$ at $\Delta\overline{T}_*$ equal to 10^{-3} (curve 1) and 10^{-2} (curve 2).

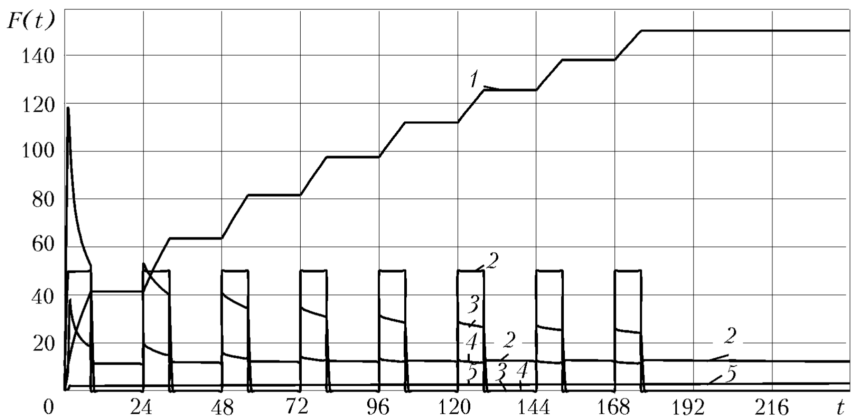

Fig. 4. Change in the heat-storage conditions during the first ten-day-period cycle. $F(t)$ corresponds to Ei, 10^7 J (1); T_0, $^{\circ}$C (2); q_0, 10 W/m^2 (3); A_m (4); R, m (5). t, h.

of the expansion terms conclusively clarifies the situation. It was established that in the region of the highest temperatures ($r < R_*$) the temperature potential at a fixed point r = const does not change with time at large values of A_m under practically steady-state operating conditions. In other words, the introduced energy with a potential of the order of 50°C is practically entirely transferred through the high-temperature region and is converted into heat with a potential close to the potential of the ground mass T_m. To obviate such negative consequences, it is necessary to control the heat introduction. The control reduces to the restriction of R and the increase of the "filling" of the temperature profile. The latter can be done only by decreasing q_0.

It should be noted that the above-described features of the process impose heavy demands on the computational methods; therefore, it is difficult to directly and exactly solve Eq. (1) by any numerical method, for example, the method of finite differences.

Figure 4 shows the results of calculation of the controlled operation of the heat exchanger–ground system during the above- indicated ten-day-period cycle. The following algorithm of control was constructed within the limits of problem (9)–(14). At T_w = 50°C = const, on attainment of the value of R = 2.0 m, the boundary of the storage region R was maintained constant by control of the value of q_0 for the purpose of increasing the "filling" of the temperature profile and, as a consequence, decreasing the parameter A_m. The above-indicated ultimate value of R was attained after 1.49 h of operation (A_m = 37.04, q_0 = 1072.4 W/m^2) and was held to the end of the light day (A_m = 17.98, q_0 = 523.1 W/m^2). The termination of the heat supply after 8 h of operation decreased T_0 from 49.81 to 11.44°C, and the 16-h "drift" had the following results: R = 2.12 m, T_0 = 11.28°C. During the next light day, the storage region was maintained constant and the next "drift" led to R = 2.23 m and T_0 = 11.77°C. This procedure was repeated for eight

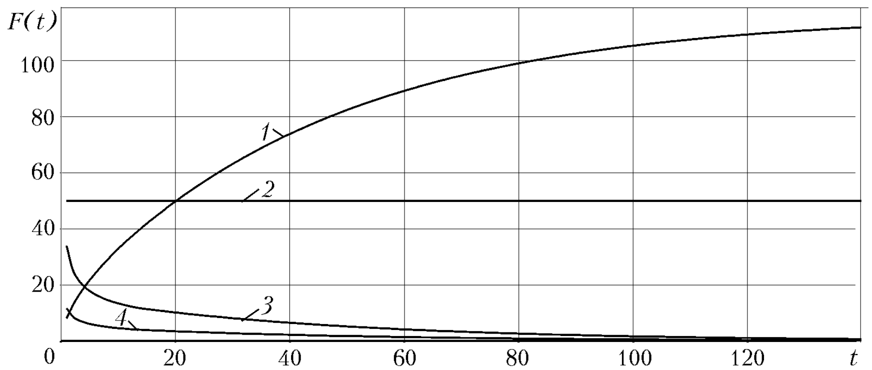

Fig. 5. Change in the conditions of the controlled heat storage in the case of continuous operation. $F(t)$ corresponds to Ei, 10^8 J (1); T_0, ^oC (2); q_0, 10 W/m^2 (3); A_m (4). t, day.

days. At the end of the last two days of "pure drift" of the first ten-day period the results were as follows: R = 3.05 m, T_0 = 12.24^{o}C. In this manner we calculated the monthly and half-year cycles. The final values were as follows: R = 9.70 m, T_0 = 11.35^{o}C, and Ei = $0.9801 \cdot 10^{10}$ J.

The aforesaid leads to the conclusion that interruptions in the operation of a heat exchanger inevitably lead to a widening of the boundaries of the storage region and, in doing so, prevent the attainment of a sufficient "filling" of the temperature profile, characterized by $A_m \sim 0$ and T_0 close to T_w. To obtain such characteristics, it is necessary to provide continuous operation of the heat exchanger, which can be attained with the use of a twenty-four hour heat-storage device. The capacity of such a heat-storage device should be 0.35 m^3/kW in order that it could heat water from 50 to 90^{o}C for 8 h for the purpose of its subsequent use as an addition to the main heat-transfer agent during the next 16 h. Figure 5 shows how the conditions of heat storage change with time in the case of such a solution. After 144 days, they were as follows: T_0 = 50.0^{o}C, R = 2.0 m, A_m = 0.216, q_0 = 6.32 W/m^2, and Ei = $0.1122 \cdot 10^{11}$ J. These values should be considered as ultimate. It should be noted that the average value of $\Delta T = (T - T_m)$ in the heat-storage ground mass, calculated by (3), cannot exceed $0.2(T_0 - T_m)$ even at a maximum "filling" of the temperature profile ($A_m = 0$). Under the conditions considered, ΔT = 8^{o}C, whereas $(T_0 - T_m)$ = 40^{o}C. Thus, storage of heat in an infinite ground mass with the use of one heat exchanger is not very efficient.

3. Analysis of Operation of a Group of Heat Exchangers. It would be reasonable to use counter heat flows to decrease the negative consequences of the spatial unboundedness of the ground mass and increase ΔT to the maximum value $(T_0 - T_m)$. This solution can be realized with the use of a group of k heat exchangers positioned, for example, in a rectangular region ($k = m \times n$) with a step L (Fig. 6). Before the heat-storage regions of each of the heat exchangers come in contact ($0 < t \le t_{i.s}$, $R(t_{i.s}) = L/2$), they operate independently of each other, and this operation period is calculated by the method described in Secs. 1 and 2. Upon the boundaries of these regions coming into contact, combined operation of the heat exchangers begins and, as a result, the heat potential of the main heat-storage region $V_o = L^2 Z(m-1)(n-1)$ increases. The heat interaction of V_o with the surrounding ground mass is realized through the buffer subregion V_s adjacent to V_o, the dimensions of which change with time and are characterized by the parameter $R_s(t)$ (Fig. 7). In what follows, we will assume that the heat loads of each of the k heat exchangers are equal (q_0 = idem). In this case, the value of q_0 should be sufficient to provide a given rate of increase in the temperature of V_o with account for the heat flow from V_o through the surface $S_o = 2L[(m-1)(n-1)L + (m+n-2)Z]$ to the surrounding ground mass. As the calculations done in Secs. 1 and 2 have shown, individual regions of heat storage come into contact after one or two hours of operation, when the temperature changes abruptly and the initial thermodynamic potential transforms into the potential of the external ground mass. Therefore, the heat flowing from the peripheral heat exchangers to the region external relative to V_o is irretrievably lost. We will assume that it functions as a heat screen along the edges of the parallelepiped V_o. Thus, even at the beginning of the process the heat efficiency of a group of heat exchangers is

$$\eta_{h,g} = 1 - \frac{m+n-1}{mn} . \tag{16}$$

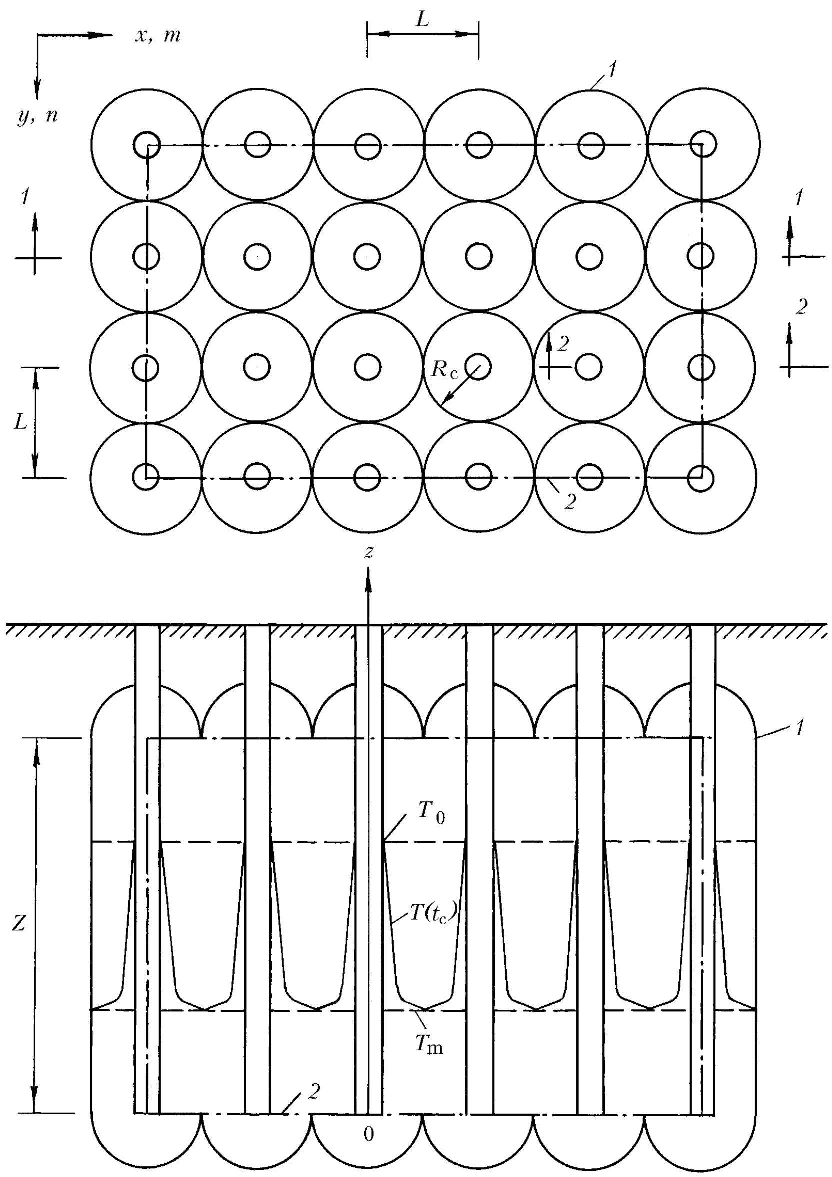

Fig. 6. Plan and section 1–1 of a group of heat- exchangers: 1) boundary of heat propagation at the instant t_c. 2) boundaries of V_o.

The value of $\eta_{h,g}$ increases with increase in m and n.

Let us construct the basic computational dependences by the method described in Sec. 1. At $t > t_c$ the temperature profile in the process of heat transfer from the heat exchangers to the region V_o should encounter conditions analogous to conditions (2), except for the fourth condition, with a space limitation $R = R_c = L/2$, which leads to the expressions

$$\frac{T - T_{ñ}}{T_0 - T_{ñ}} = \begin{cases} (1-\kappa)^2 (1 + 2\kappa - A_{ñ}\kappa) & \text{at} \quad 0 \le A_{ñ} \le 3 \, ; \\ (1-\kappa)^{A_{ñ}} & \text{at} \quad 3 < A_{ñ} \le \infty \, , \end{cases} \tag{17}$$

where

$$\kappa = \frac{r - R_0}{R_{ñ} - R_0} \, ; \quad A_{ñ} = \frac{q_0 \, (R_{ñ} - R_0)}{\lambda_m \, (T_0 - T_{ñ})} \, ;$$

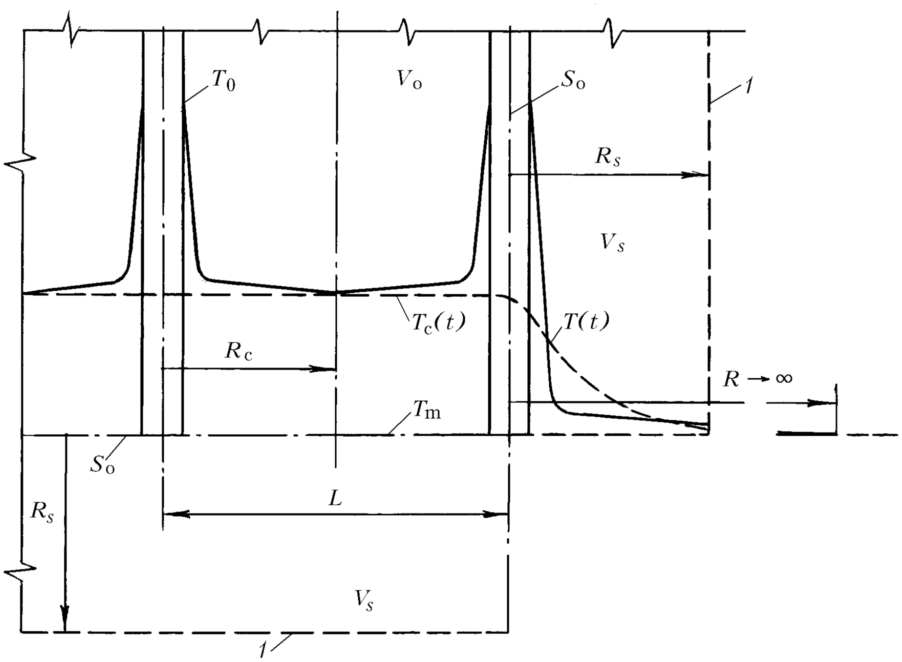

Fig. 7. Section 2–2 of the plan (see Fig. 6) and temperature distribution in the ground mass at $t > t_c$: 1) outer boundary of V_s.

$$\frac{dT_0}{dt} = a_m \frac{(T_{\text{ñ}} - T_0)}{(R_{\text{ñ}} - R_0)} \left[\frac{6 - 4A_{\text{ñ}}}{(R_{\text{ñ}} - R_0)} + \frac{A_{\text{ñ}}}{R_0} \right] \quad \text{at} \quad 0 \le A_{\text{ñ}} \le 3 \; ; \tag{18}$$

$$\frac{dT_0}{dt} = a_m \frac{(T_{\text{ñ}} - T_0)}{(R_{\text{ñ}} - R_0)} \left[\frac{A_{\text{ñ}} (1 - A_{\text{ñ}})}{(R_{\text{ñ}} - R_0)} + \frac{A_{\text{ñ}}}{R_0} \right] \quad \text{at} \quad 3 < A_{\text{ñ}} \le \infty \; .$$

Heat interaction of the region V_0 with the external ground mass occurs in the case where the following conditions are fulfilled, respectively, at the inner and outer boundaries of the buffer subregion V_S:

$$u = 0: \quad T = T_{\text{ñ}} \, , \quad \frac{\partial T}{\partial u} = 0 \; ;$$

$$u = R_s: \quad T = T_m \, , \quad \frac{\partial T}{\partial u} = 0 \, , \quad \frac{\partial^2 T}{\partial u^2} = 0 \qquad (u = x, y) \; . \tag{19}$$

The following relation satisfies these conditions:

$$\frac{T - T_m}{T_{\text{ñ}} - T_m} = (1 - \psi)^3 (1 + 3\psi) \, , \quad \psi = \frac{u}{R_s} \qquad (u = x, y) \; . \tag{20}$$

Here, u is measured along the normal to S_0 from S_0 to the region external relative to V_0.

The heat balance of one cell ($L \times L \times Z$) of the group per unit height of the cell is

$$2\pi R_0 q_0 = L^2 \rho_m c_m \frac{dT_{\text{ñ}}}{dt} + \frac{d}{dt} \int_{R_0}^{R_{\text{ñ}}} 2\pi \rho_m c_m (T - T_{\text{ñ}}) \, r dr + 2L \left(\frac{L}{Z} + \frac{1}{m-1} + \frac{1}{n-1} \right) q_s \, , \tag{21}$$

where q_s is the density of the heat flow absorbed by the buffer subregion V_s. The integral in (21) is easily calculated with the use of distribution (17). It should be emphasized that the heat-balance condition (21) is true for each cell, including the corner one, since the expression before q_s accounts for the contribution of each cell to V_o, which provides a uniform distribution of T_c over the entire region V_o.

The heat content of the buffer subregion per unit S_o is determined, in accordance with (20), by the expression

$$\mathrm{Ei}_s = \int_0^{R_s} \rho_m c_m (T - T_m)\, du = 0.4 \rho_m c_m (T_{\tilde{n}} - T_m) R_s\,. \tag{22}$$

In the case where Ei_s remains unchanged,

$$\frac{dR_s}{dt} = -\frac{R_s}{(T_{\tilde{n}} - T_m)} \frac{dT_{\tilde{n}}}{dt}\,. \tag{23}$$

At the same time, at $A_m = 0$ we may write, in accordance with (20) and (1), an expression similar to (11):

$$\frac{dT_{\tilde{n}}}{dt} = -12 a_m \frac{(T_{\tilde{n}} - T_m)}{R_s^2}\,. \tag{24}$$

On substitution of (24) into (23) and integration, we obtain

$$R_s = \sqrt{24 a_m (t - t_{\tilde{n}})}\,. \tag{25}$$

Since the function T_c changes from T_m to $T_c \approx T_w$ during a half-year period of heat storage and, accordingly, Ei_s changes slowly, expression (25) can be used in the first approximation without any limitations. In this case, differentiation of (22) gives a formula for $q_s(t)$:

$$q_s = 0.4 \rho_m c_m \left[12 a_m \frac{(T_{\tilde{n}} - T_m)}{R_s} + R_s \frac{dT_{\tilde{n}}}{dt} \right]. \tag{26}$$

Substituting (26) into (21), we find a unique dependence of $T_c(t)$ on the density of the heat flow from the heat exchangers q_0 and, from formula (25), determine the value of $R_s(t)$ in the process of energy introduction.

The temperature profile does not change when heat exchangers cease to operate ($q_0 = 0$) since its "filling" is maximum in the buffer subregion. The rate of change in $T_c(t)$ is determined by Eq. (24). The condition of invariability of the stored energy is as follows:

$$\frac{\partial}{\partial t}\left[S_{\hat{\imath}} \int_0^{R_s} (T - T_m)\, du + V_{\hat{\imath}} (T_{\tilde{n}} - T_m) \right] = 0\,. \tag{27}$$

Substitution of (20) into (27), integration with respect to u, and subsequent differentiation with respect to t make it possible to find, with the use of (24), an equation for $R_s(t)$:

$$\frac{dR_s}{dt} = \frac{12 a_m}{R_s^2} \left(R_s + \frac{V_{\hat{\imath}}}{0.4 S_{\hat{\imath}}} \right) \tag{28}$$

and, in doing so, complete the determination of the change in the main parameters of this part of the problem.

Figure 8 presents the results of calculation of the heat storage in the ten-day-period regime with the use of a group of coaxial heat exchangers ($m = n = 6$, $L = 5$ m, $\eta_{h,g} = 0.695$) with design dimensions indicated in Sec. 2 in the case where T_c tends to a finite value equal to $\sim 50^{o}$C and $q_0 = 5 \cdot 10^3$ W/m^2 = const. It should be noted that T_c constantly increases despite the fact that it somewhat decreases in the drift periods. The dimension of the buffer subre-

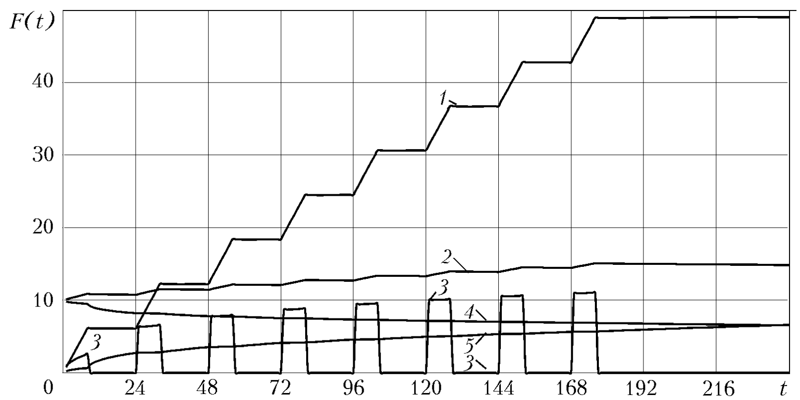

Fig. 8. Change in the conditions of heat storage with the use of a group of heat exchangers. $F(t)$ corresponds to Ei, 10^{10} J (1); T_c, ^oC (2); q_0, 10 W/m^2 (3); $\eta_o \cdot 10$ (4); R_s, m (5). t, h.

gion reaches the value of R_s = 6.60 m toward the end of the first ten-day period. Clearly, with increase in R_s, the energy ratio in V_s and in the main volume V_o changes in favor of V_s. At the beginning of the heat-storage process, $\eta_o = \mathrm{Ei}_o/\mathrm{Ei} = 1$, and η_o decreases to 0.654 toward the end of the first ten-day period. It was established that at $q_0 = 5 \cdot 10^3$ W/m^2, the energy introduction is completed ($T_c \approx 50^oC$) on the fifth day of the 14th ten-day period (R_s = 18.39 m, q_s = 208 W/m^2, Ei = $0.665 \cdot 10^{13}$ J, and η_o = 0.405). Such a value of T_c can be attained toward the end of the 18th ten-day period at a heat flow density of $q_0 = 3.9 \cdot 10^3$ W/m^2 (R_s = 20.85 m, q_s = 169.8 W/m^2, Ei = $0.688 \cdot 10^{13}$ J, η_o = 0.3748). It should be remembered that R_s determines the value of $h(t)$ (see Fig. 1).

CONCLUSIONS

Our numerical investigations undoubtedly point to the fact that heat storage with the use of a group of heat exchangers is more preferential than heat storage with the use of a single exchanger. The main advantages are as follows: (a) there is no need to use twenty-four-hour heat-storage devices; (b) there is no need for strong control over the process; (c) the quality of the stored energy substantially increases since the quantity η_o characterizing its temperature potential can be 0.4–0.5 or higher, whereas $\eta_o = 0$ in the case of heat storage with the use of a single heat exchanger.

Our calculations should be considered as an example of realization of the computational method. Both the initial and final values can be different depending on the characteristics of the concrete equipment and the limitations imposed on the functions. However, the above-mentioned advantages of the "group" solution remain true.

The simple and fairly exact method proposed makes it possible to perform simulations of the dynamics of ground heat storage with time interruptions in the case where a single heat exchanger is used and in the case where heat storage is performed continuously with the use of a group of heat exchangers. As follows from the analysis done in Sec. 2, it is difficult to directly solve Eq. (1) by the method of finite differences.

NOTATION

A, parameter; a, thermal diffusivity, m^2/sec; c, specific heat, J/(kg·K); Ei, energy, J; G, flow rate of the intermediate heat-transfer agent, kg/sec; H, heat-insulated region of the heat exchangers (Fig. 1), m; h, protective ground layer (Fig. 1), m; k, number of heat exchangers in a group; L, step, m; m and n, number of heat exchangers in the rows parallel to the x and y axes; N, power of the external source, W; q, heat-flow density, W/m^2; R, radius (linear dimension) of heat propagation, m; S, area of the heat-transfer surface, m^2; T, temperature, ^oC, K; $\check{T}$, mean-integral temperature, ^oC, K; t, time, sec; V, volume, m^3; v, velocity, m/sec; x, y, z, r, coordinates, m; Z, operating height of a heat exchanger, m; α, heat-transfer coefficient, W/(m^2·K); λ, heat conduction, W/(m·K); η, dimensionless coordinate; ζ, hydraulic resistance coefficient; ρ, density, kg/m^3. Subscripts: 0, parameters at $r = R_0$; w, water; e, end; m, mass; b, beginning; o, main; c, parameters in the case of combined operation of heat exchangers; h, heat; i.s, on the inner surface of a heat exchanger; g, group of k heat exchangers; s, quantities measured from S_o; *, particular.

REFERENCES

1. A. V. Luikov, *Heat and Mass Transfer: Handbook* [in Russian], Énergiya, Moscow (1971).
2. A. I. Nakorchevskii, Conjugate problems of unsteady heat and mass conduction under varying external conditions, *Inzh.-Fiz. Zh.*, **72**, No. 4, 782–791 (1999).
3. L. G. Loitsyanskii, *A Laminar Boundary Layer* [in Russian], Fitmatgiz, Moscow (1962).